Updated geology and porphyry copper potential of the Klaza deposit, Mount Nansen district (Yukon MINFILE 115I 067)

W.-S. Lee*, D.J. Kontak and J.P. Richards†
Harquail School of Earth Sciences, Laurentian University

P. Sack
Yukon Geological Survey

Lee, W.-S., Kontak, D.J. Richards, J.P. and Sack, P., 2020. Updated geology and porphyry copper potential of the Klaza deposit, Mount Nansen district (Yukon MINFILE 115I 067). *In:* Yukon Exploration and Geology 2019, K.E. MacFarlane (ed.), Yukon Geological Survey, p. 75–97.

Abstract

Porphyry to epithermal deposit models are inferred to best describe the Late Cretaceous Klaza Au-Ag-Pb-Zn-(Cu) deposit. Here we report evidence for a protracted and complex magmatic-hydrothermal system typical of porphyry-epithermal deposits (e.g., multiple magmatic events, magma mingling, relevant vein-alteration types). In the Klaza area, there are at least four compositionally and texturally distinct intrusions interpreted as part of the Casino intrusive suite (ca. 80–76 Ma) that intrude granodiorite country rock of the Whitehorse suite (ca. 105 Ma). A ca. 72 Ma dike swarm (likely Prospector Mountain suite) was emplaced approximately 4–5 m.y. after emplacement of the Casino suite. Evidence of high-T hydrothermal activity consists of early dark micaceous (EDM) veins, sinuous and planar A-type veins, B-type, and D-type veins, and molybdenite-quartz veins. Composite epithermal-type sulphide veins cut high-T Cu-Au-Mo mineralization associated with phyllic and lesser potassic alteration assemblages. The age of porphyry-type mineralization is constrained by ^{187}Re-^{187}Os molybdenite dating to ca. 77 Ma (Kelly) and ca. 71 Ma (Cyprus). The ^{40}Ar-^{39}Ar muscovite dates from phyllic alteration in the Central Klaza zone yield ages of ca. 77 Ma. These field observations, integrated with archival Cu-Au-assay data, suggest the Klaza epithermal veins are located in the phyllic alteration shell of a two-stage Cu-Au-Mo porphyry system. It is possible that the Klaza epithermal veins represent a Prospector Mountain-age porphyry–epithermal system overprinting a Casino-age porphyry system.

* wlee1@laurentian.ca

† deceased, June 7, 2019

Introduction

The Late Cretaceous Klaza Au-Ag-Pb-Zn-(Cu) deposit is located within the historic Mount Nansen gold camp (MNGC; Fig. 1), 70 km from the village of Carmacks, Yukon. It has a current combined (indicated and inferred) mineral resource of 4.457 Mt of 4.8 g/t Au, 98 g/t Ag, 0.7% Pb, and 0.9% Zn (Ross et *al*., 2018). The dominant mineralization style at Klaza consists of 0.2 to 8 m wide polymetallic veins having drill-indicated strike lengths of 300 to 2500 m and vertical depths from surface of at least 500 m (Turner and Dumala, 2016). This vein system has been compared to the past-producing Brown McDade/Mount Nansen veins and to a porphyry to epithermal model for the MNGC (Hart and Langdon, 1997; Mortensen et *al*., 2016). This paper provides new geological insights into the current understanding of the Klaza deposit model as supported by new geochronologic data and supporting field constraints (work done in 2017 and 2019), with derived paragenetic reconstructions based on field and petrographic observations in addition to assessing metal zonation at the deposit scale. This information is collectively used to assess the metal endowment of Klaza and its potential as a porphyry-type deposit.

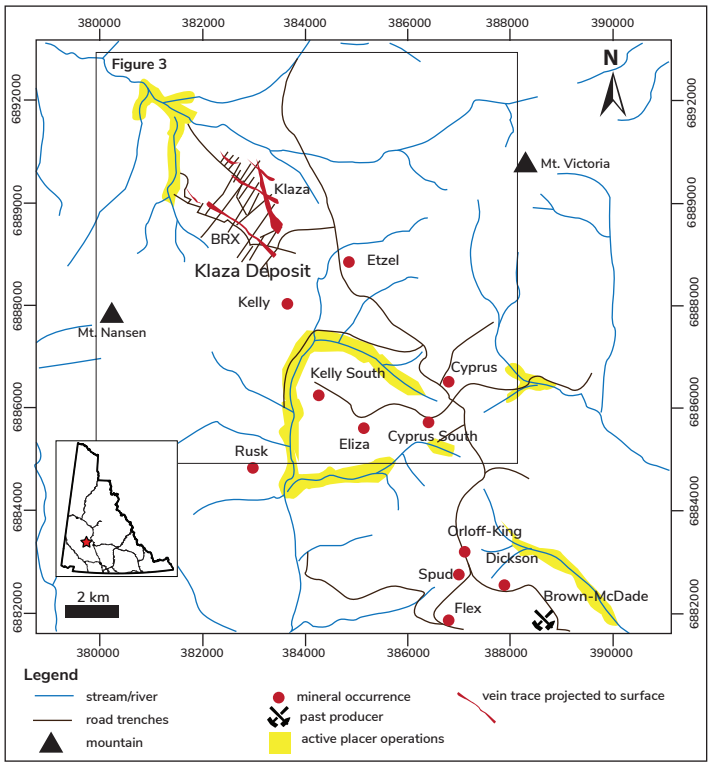

Figure 1. *Geographic map of Klaza–Mt. Nansen district displaying placer-bearing streams (Yukon Mining Recorder placer claim map sheet 115I03P), mineral occurrences, and roads.*

Regional geology

The MNGC is located in the southeastern end of the Dawson Range gold belt (Fig. 2) which stretches from the Yukon-Alaska border to within 50 km of the town of Carmacks, Yukon (Allan et *al*., 2013). Basement rocks in the MNGC comprise Devonian and older metamorphosed volcaniclastic and sedimentary rocks of the parautochthonous Yukon-Tanana terrane, accreted to the Laurentian margin between the Late Triassic and Early Jurassic, during east-dipping subduction (Allan et *al*., 2013; Nelson et *al*., 2013). This subduction event emplaced the regionally extensive Long Lake suite and Minto suite plutons. Porphyry-type systems, such as Minto (60 Mt at 1% Cu and 0.4 g/t Au; Allan et *al*., 2013) and Carmacks Copper (15.69 Mt oxide at 1% Cu, 0.4 g/t Au, and 4 g/t Ag; 8.07 Mt sulphide at 0.7% Cu, 0.2 g/t Au, and 2.3 g/t Ag; Kovacs et *al*., 2017), formed around the Late Triassic (Kovacs et *al*., *in press*).

Renewed east dipping subduction led to the emplacement of the *ca*. 105 Ma Dawson Range batholith (Whitehorse plutonic suite; 112–98 Ma) and the coeval Mount Nansen volcanic package in the mid-Cretaceous (115–110 Ma; Klöcking et *al*., 2016). Continued east-dipping subduction in the Late Cretaceous led to the emplacement of the Casino plutonic suite (78–74 Ma) and related cluster of porphyry-epithermal systems (Casino, Cash, Nucleus, Revenue, Sonora Gulch) within the Dawson Range belt (Allan et *al*., 2013; Nelson et *al*., 2013). The Casino plutonic suite is less voluminous than the Whitehorse suite, although it occurs regionally throughout the Dawson Range gold belt in the form of porphyritic dikes and stocks. The most economically important of these is the Patton porphyry, which is associated with the Casino porphyry deposit (1057 Mt at 0.2% Cu, 0.23 g/t Au and 0.022% Mo; Allan et *al*., 2013). Quartz-feldspar-porphyry (QFP) dikes yielding ages of 77–74 Ma are also reported at Sonora Gulch, the Freegold district, and the Mount Nansen district (Allan et *al*., 2013; Bennett, 2010; Bineli-Betsi and Bennett, 2010; Bineli-Betsi et *al*., 2013; Mortensen et *al*., 2016).

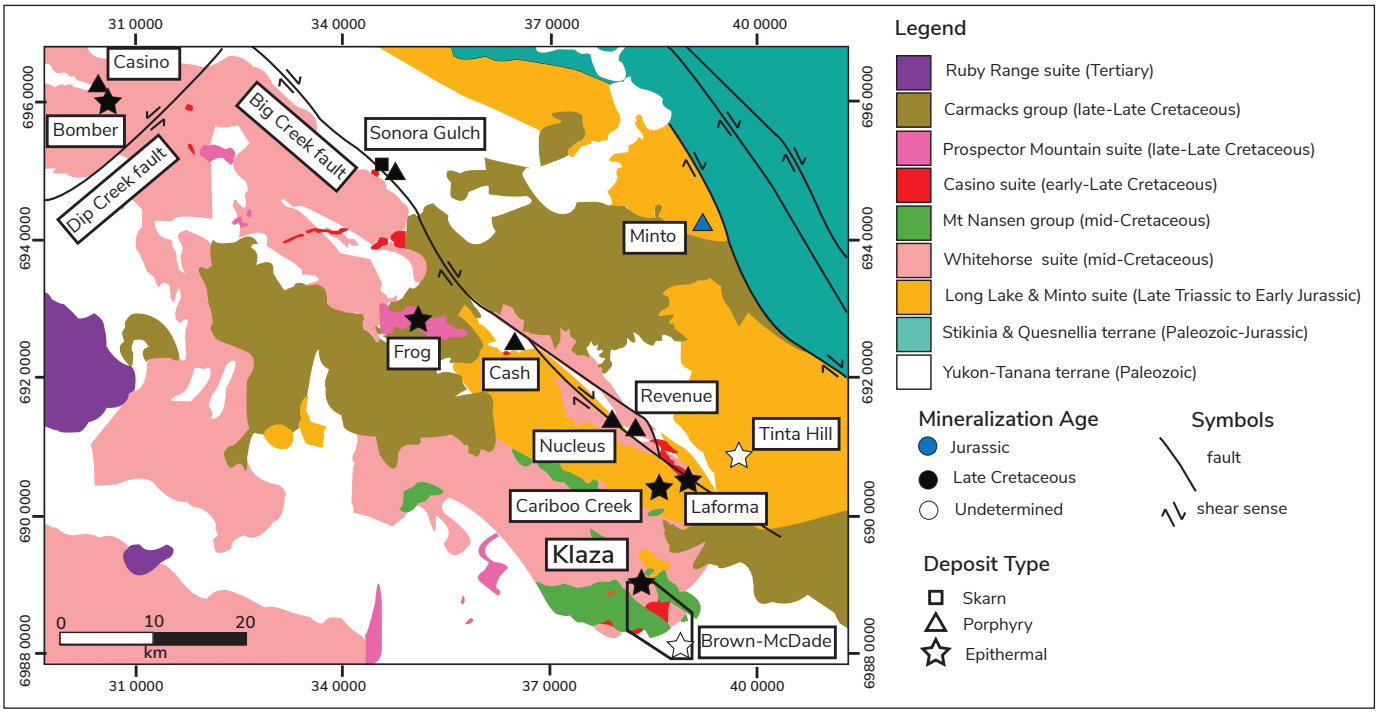

Figure 2. *Regional geologic map of the mid to southern Dawson Range, Yukon. UTM Zone 08, Datum: NAD 83. Map modified from Yukon Geological Survey digital map version April 2018.*

Soon after emplacement of the Casino suite, the composition of the magma became slightly more alkalic; it consists of both volcanic (Carmacks group) and shallow plutonic (Prospector Mountain suite) components. The Prospector Mountain suite and the coeval porphyry-epithermal prospects of Frog and Lilipad were emplaced from 69–67 m.y. (Allan et *al.*, 2013). Several porphyry-epithermal systems of Late Cretaceous age are localized on, or near, the Big Creek fault, a northwest trending transcrustal structure located on the northern margin of the Dawson Range batholith. Systems farther away from the fault, such as Casino, Tinta Hill and Klaza–Mt. Nansen display the same northwest structural trends.

Methodology

Ten days of fieldwork were conducted in August 2019 comprising: (1) re-logging and sampling of Cu-rich archival drill core from the eastern part of the deposit; and (2) traverses to the northeast and southwest extents of the Klaza property. Representative samples of least altered and altered intrusive rocks were cut and stained for K (*i.e.*, K-feldspar, biotite, sericite) using cobaltinitrite staining at a commercial lab. Least altered and weathered intrusive rock samples were from core drilled far from mineralization or found in trenches across the property. Images of the stained rocks were processed utilizing Image J software to estimate abundance of plagioclase, quartz, and K-feldspar. A preliminary classification of the intrusive rocks is made based on the modal mineralogy. Sulphide paragenesis and element distribution in vein stages were investigated using a combination of optical microscopy, SEM-EDS, and LA-ICP-MS analysis, the detailed results of which will be presented elsewhere.

We present an updated geologic map for the Klaza area in Figure 3a. Structure is constructed from a combination of drillhole constraints and VLF-IP data (very low frequency electromagnetic survey and induced polarization survey; Fig. 3b). Limitations in geological and geophysical information are highlighted in Figure 3c. Outcrop and subcrop information from Klöcking et *al.* (2016) and Ryan et *al.* (2016) were combined with data from this study. Outcrop and subcrop data are highlighted in bold colours whereas interpretive geology is indicated in pale colours. Magnetic (reduced to pole, first vertical derivative,

and magnetic susceptibility; Ross *et al.*, 2018), electromagnetic (very-low-frequency-EM; Fig. 3b), and induced polarization (IP) geophysical data from Ross *et al.* (2018) were utilized to define lithologic boundaries and faults/lineation. The first unit intersected in diamond drill holes were also used to construct this surface map within drilling extents.

Deposit geology

The area around the Klaza deposit was not subjected to Pleistocene glacial erosion and thus the landscape is mostly deeply weathered rolling hills with >20–30 m of overburden in valleys. The Klaza deposit is entirely buried and only "outcrops" in exploration trenches. Hart and Langdon (1997) propose that the Klaza deposit sits within an uplifted block of a horst structure, with mid-Cretaceous Mount Nansen volcanic rocks preserved on either side. Bounding faults of the horst block run parallel to mineralized trends as well as regional structural trends and are inferred to be pre-mineralization faults (Klöcking *et al.*, 2016). The Hart and Langdon (1997) model also highlights northeast-trending faults that crosscut and offset the host block with its associated bounding faults. Ryan *et al.* (2016) proposed a map that showed the NW-trending faults as the dominant structure in the Klaza area but showed little evidence of the NE-faults.

The geological map in Figure 3 shows northwest and northeast structural trends. The NW trend comprises dikes and faults in the main deposit and includes the composite veins. The veins occupy Riedel splays from dextral strike-slip movement on the faults. The NE-trending faults cut and sinistrally displace the NW trends, thus dividing the deposit into the western, central and eastern blocks. The eastern block and the western block are interpreted to be uplifted relative to the central block. The magnitude of this vertical displacement is unknown.

The Klaza polymetallic veins spatially coincide with 77–76 Ma quartz-feldspar porphyritic (QFP) dikes (Mortensen *et al.*, 2016; Turner and Dumala, 2017). The QFP dikes and the Klaza veins are hosted in the mid-Cretaceous (*ca.* 107 Ma) Whitehorse suite granodiorite, part of the regionally extensive Dawson Range batholith emplaced between 115 and 105 Ma (Allan *et al.*, 2013). The deposit is divided into four main resource zones: Central Klaza, Central BRX, Western Klaza and Western BRX respectively. The epithermal type mineralization seen in base-metal-rich veins transitions into Au-Cu-Mo-rich stock work veins and veinlets towards the Kelly and Cyprus porphyry prospects in the southeast.

Intrusive and extrusive rocks

The intrusive suites discussed below are assigned a map unit, whereas each intrusive phase intersected in drill core is assigned a short-form numbered code (i1–i5) for simple referencing to the observed paragenetic sequence.

Minto suite (LTrEJgM)

Intrusive rocks from this suite are observed in outcrop north-northeast of the Klaza deposit where they unconformably underlie Mt. Nansen Group volcanic rocks and are intruded by Whitehorse suite plutonic rocks. Slightly older (*ca.* 211 Ma) rocks of the Minto suite are also documented to unconformably underlie the Mt. Nansen Group rocks to the west and southwest of the Klaza deposit, where they intrude the Snowcap assemblage (Klöcking *et al.*, 2016). The composition of these of rocks varies between quartz monzodiorite and tonalite, and contain coarse to medium-grained, foliated hornblende and biotite (Allan *et al.*, 2013; Kovacs *et al.*, 2016). The outcrop of this suite, observed to the northeast of the Klaza deposit (Fig. 3a), is medium to coarse-grained porphyritic foliated hornblende-granodiorite with K-feldspar phenocrysts. Magnetic susceptibility for this suite ranges from ~15 to 25 nT.

Mt. Nansen group (mKN)

The Mt. Nansen volcanic complex outcrops to the east and west of the Klaza deposit, often forming knobs, tors and talus slopes. Exposure to the east and southeast of the Klaza deposit was mapped at 1:15 000-scale by Klöcking *et al.* (2016). Klöcking *et al.* (2016) suggest the volcanic stratigraphy is upright, undeformed, and dips at an angle of ~45–60° to the northeast. This volcanic package consists of andesitic flows, breccia, and rhyolite tuffs. Constrained to a minimum thickness of 450 m, significant uplift is interpreted to have occurred with the emplacement of the Whitehorse

suite plutonic rocks (Klöcking et *al.*, 2016). Mt. Nansen group rocks are characterized by dark blocky, rock piles resistant to weathering. The andesite flows are porphyritic with large plagioclase phenocrysts and fine-grained pyroxene-bearing groundmass. Outcrops on Victoria Mountain suggest flat-lying stratigraphy in this package to the east of the Klaza deposit (Fig. 3a). Magnetic susceptibility for the Mt. Nansen group rocks ranges between ~20 and 50 nT, making it highly pronounced in magnetic surveys. A detailed description of this volcanic package is documented in Klöcking et *al.* (2016).

Whitehorse suite (mKWg)

i1: Biotite-hornblende granodiorite to tonalite

The Whitehorse suite granodiorite, dates at *ca.* 107.9 Ma on the property (Mortensen et *al.*, 2016), is the most abundant rock type observed in drill core, and is the main host to the epithermal mineralization.

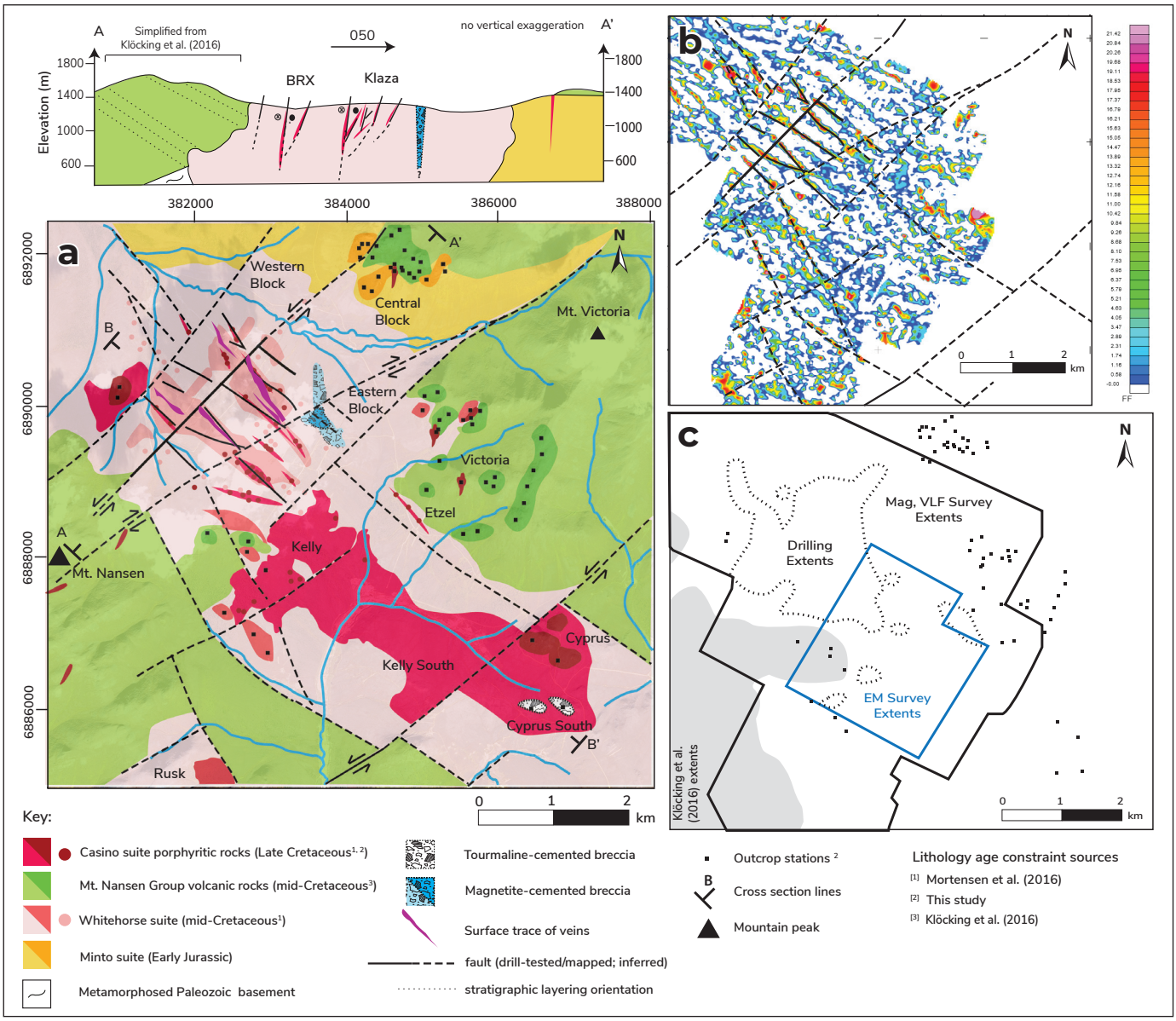

Figure 3. (a) *Geologic map of the Klaza deposit. Outcrop traces and "top of drillhole" intercepts are highlighted in bold colours while interpretative geology is indicated by pale colours. UTM Zone 08, Datum: NAD 83.* ***(b)*** *VLF-IP map highlighting shallow conductors and permeable fault zones. Interpretive and drill-tested faults are overlain on the geophysical map.* ***(c)*** *A limits of confidence map indicating sources of information for constraining the geological map.*

It is a composite intrusion and two dominant phases are identified: (1) a biotite-amphibole phyric granodiorite (Fig. 4a,b); and (2) biotite tonalite (Fig. 4c,d). Both phases consist of large, euhedral plagioclase (30–45%) phenocrysts in addition to subhedral quartz (25–40%) which has a bimodal size range, subhedral K-feldspar (0–20%) and intergranular biotite (10–15%) and amphibole (0–8%). Dioritic autoliths are a common occurrence in this suite. In two of these phases, there are larger subround (*i.e.*, corroded) quartz phenocrysts. Petrography shows accessory zircon, epidote, titanite and chlorite after biotite. This suite is commonly altered exhibiting a light propylitic overprint of chlorite, epidote and carbonate. Magnetic susceptibility for this suite ranges from ~15 to 20 nT.

Leucogranite/ Aplite dikes

This phase, which is seen in outcrop and drill core, consists of dikes crosscutting the i1 phase. The dikes consist of a massive, fine-grained pinkish K-feldspar-quartz-rich assemblage, and are 10 cm to 1 m thick. These aplite dikes match descriptions of a similar phase in Friend et *al.* (2018) and are inferred to be a late stage of the mid-Cretaceous Dawson Range batholith.

Casino suite (LKpC)

Casino suite rocks at the Klaza deposit occur as a composite dike swarm having a minimum of four phases (i2 to i4, see below). Magnetic susceptibility for Casino suite rocks at Klaza are between 1 and 5 nT, which manifests as mag-lows in geophysical surveys. The majority of the Casino suite rocks in the deposit record phyllic alteration as reflected by the growth of muscovite uniformly seen throughout samples studied petrographically. The consequence of the latter is the addition of K to the system, which resulted in a pervasive yellow colour to the stained rocks.

i2: Monzogranite to granodiorite

This phase occurs in the southeastern part of the Klaza property and is seen to be in sharp contact with the i1 phase. It is leucocratic, medium-grained, containing plagioclase (40%), quartz (30%) and K-feldspar (30%). It generally has a seriate texture, but plagioclase is slightly coarser and partly porphyritic (Fig. 5a). It has moderate to intense phyllic (muscovite-quartz-pyrite) and potassic (K-feldspar) alteration.

i3a: Biotite-plagioclase porphyritic granodiorite (80–78 Ma)

This phase is constrained to ca. 79 Ma (Lee et *al.*, in prep), and also occurs in the southeastern part of the Klaza property. A phase having similar texture and mineralogy is observed at the Cyprus porphyry prospect (Figs. 1 and 3). It consists of euhedral to subrounded, partially resorbed phenocrysts of plagioclase (20%), quartz (30%), and euhedral biotite (8%) phenocrysts, in a fine-grained K-rich (40%), quartz-plagioclase groundmass (Fig. 5b). The plagioclase crystals also display variable degrees of albitization. This phase maintains both sharp and gradational contacts with i2 and i3b (see below) and shows a mutual intrusive relationship with i3b as both occur in each other (Fig. 6a,b,c). Therefore, it is likely that i3a and i3b are comagmatic. This phase is variably altered and when altered can look like i4 (see below).

i3b: Hornblende-plagioclase diorite

This phase is also found in the southeastern part of the Klaza property. It is medium-grained and equigranular, and consists of plagioclase (50%), hornblende (30%) and variable biotite (5–11%). Biotite has an acicular habit (Fig. 5c). Phase i3b has variable phyllic alteration (muscovite-quartz-pyrite) and can be strongly sulphidized (*i.e.*, increase in sulphide mineral phases) due to the high amount of mafic minerals in the groundmass.

i4: Feldspar-quartz-biotite porphyritic granodiorite dikes (77–76 Ma)

This dike phase is the most commonly intersected phase of the Casino suite and is ca. 77 Ma (Mortensen et *al.*, 2016; Lee et *al.*, in prep). It is found throughout the Klaza property. Importantly, this phase is commonly co-spatial with, and cut by, composite epithermal-type veins. Phase i4 is texturally and mineralogically similar to the i3a phase, has partially resorbed plagioclase (25–30%) and quartz (15%) phenocrysts in a fine-grained K-rich (30–55%) groundmass of plagioclase

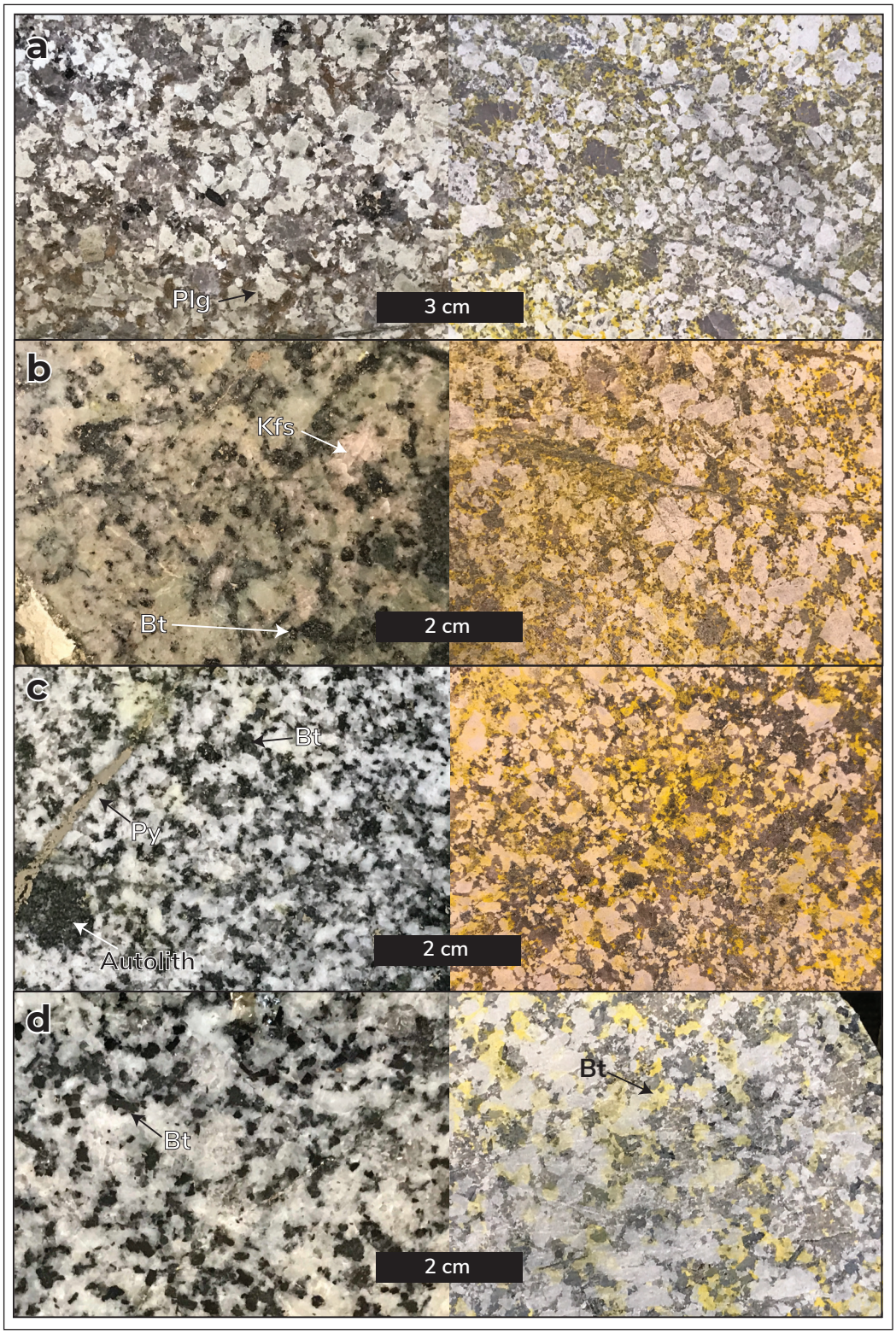

Figure 4. *Variations of the Whitehorse plutonic suite (i1 phase) at the Klaza deposit. Polished slabs are displayed on the left whereas potassium-stained slabs are displayed on the right. Note that a significant proportion of potassium staining is attributed to biotite in addition to K-feldspar.* **(a)** *Hornblende-biotite granodiorite showing significant clay-alteration.* **(b)** *Hornblende-biotite granodiorite shows light propylitic overprint.* **(c)** *Biotite-hornblende tonalite. shows light potassic (biotite) overprint.* **(d)** *Least altered biotite-hornblende tonalite. Mineral abbreviations in accordance with Whitney and Evans (2010).*

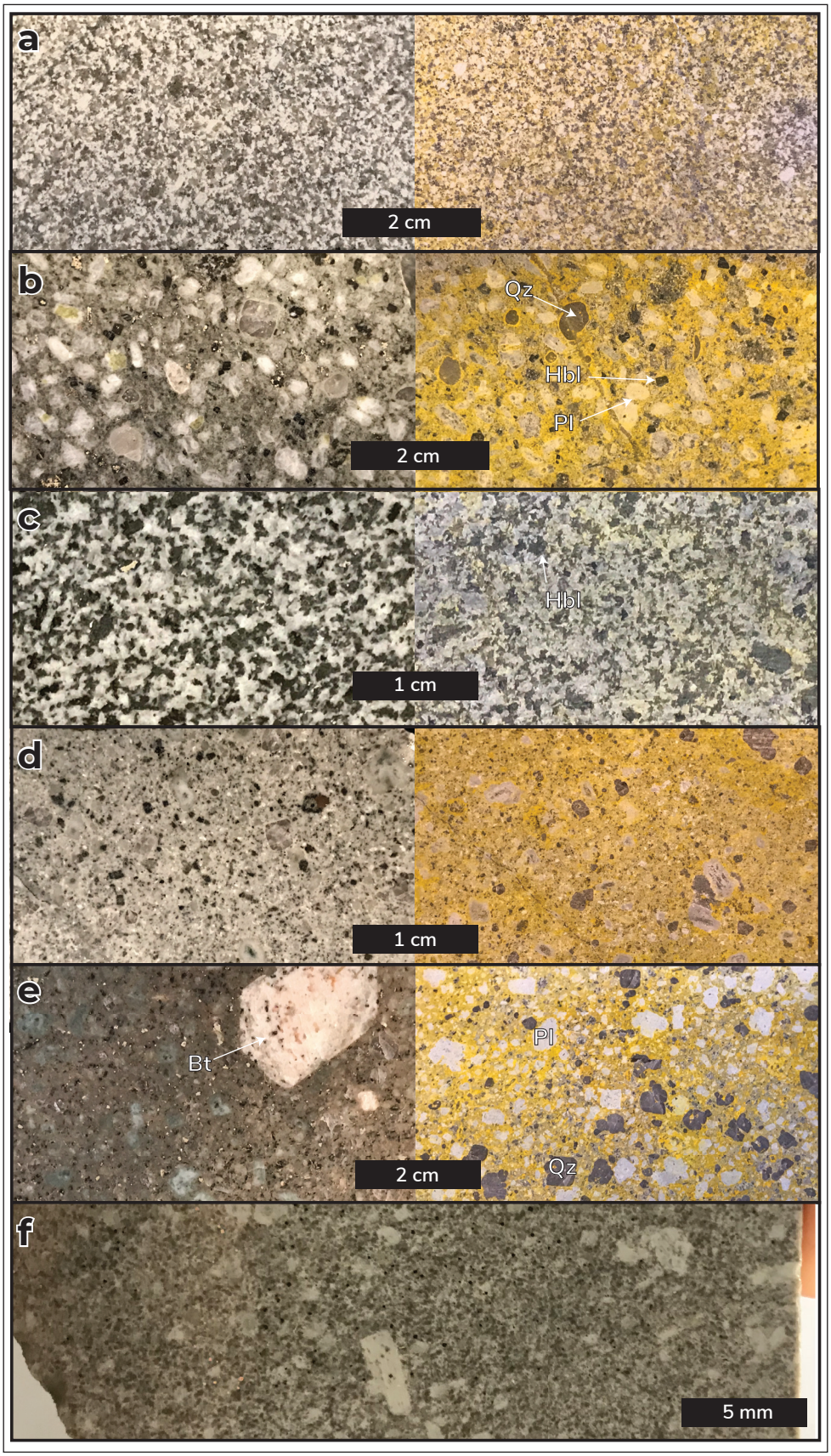

Figure 5. *Casino suite intrusive rocks. Polished slabs are displayed on the left whereas potassium-stained slabs are displayed on the right.* ***(a)*** *Monzogranite (i2 phase).* ***(b)*** *Biotite-plagioclase porphyritic granodiorite to monzogranite (i3a phase).* ***(c)*** *Hornblende-plagioclase diorite (i3b phase).* ***(d and e)*** *Feldspar-quartz-biotite porphyritic andesite dikes (i4 phase).* ***(f)*** *Feldspar-biotite porphyritic andesite dikes (i5 phase). Mineral abbreviations in accordance with Whitney and Evans (2010).*

and biotite (3–8%; Fig. 5d,e). There are localized, large (2–3 cm) plagioclase phenocrysts (Fig. 5e). Phase i4 contains more quartz but less biotite than i3a. It commonly exhibits greater phyllic/argillic alteration, forming an illite-muscovite-clay, due to its close proximity to epithermal veins and large fault zones. The alteration is texturally destructive, and results in the preservation of bleached, tan coloured dikes. The dikes are commonly barren but do host pyrite after biotite due to the phyllic overprint. This phase cuts the i3 phases and porphyry-type veins, and are in turn cut by i5 and epithermal mineralization.

Prospector Mountain suite (LKyP)

i5: Feldspar-biotite porphyritic diorite dikes (72–71 Ma)

This phase is significantly less common than the i4 phase but is found throughout the Klaza property. Identification is challenging due to the texturally destructive phyllic and argillic alteration. Current observations highlight a quartz-poor mineralogy having dominantly equant feldspar (plagioclase) and biotite phenocrysts in a fine-grained groundmass (Fig. 5f). This phase contains clasts of i4 (Fig. 6d) and is constrained to *ca.* 71 Ma (Mortensen *et al.*, 2016; Lee *et al.*, in prep).

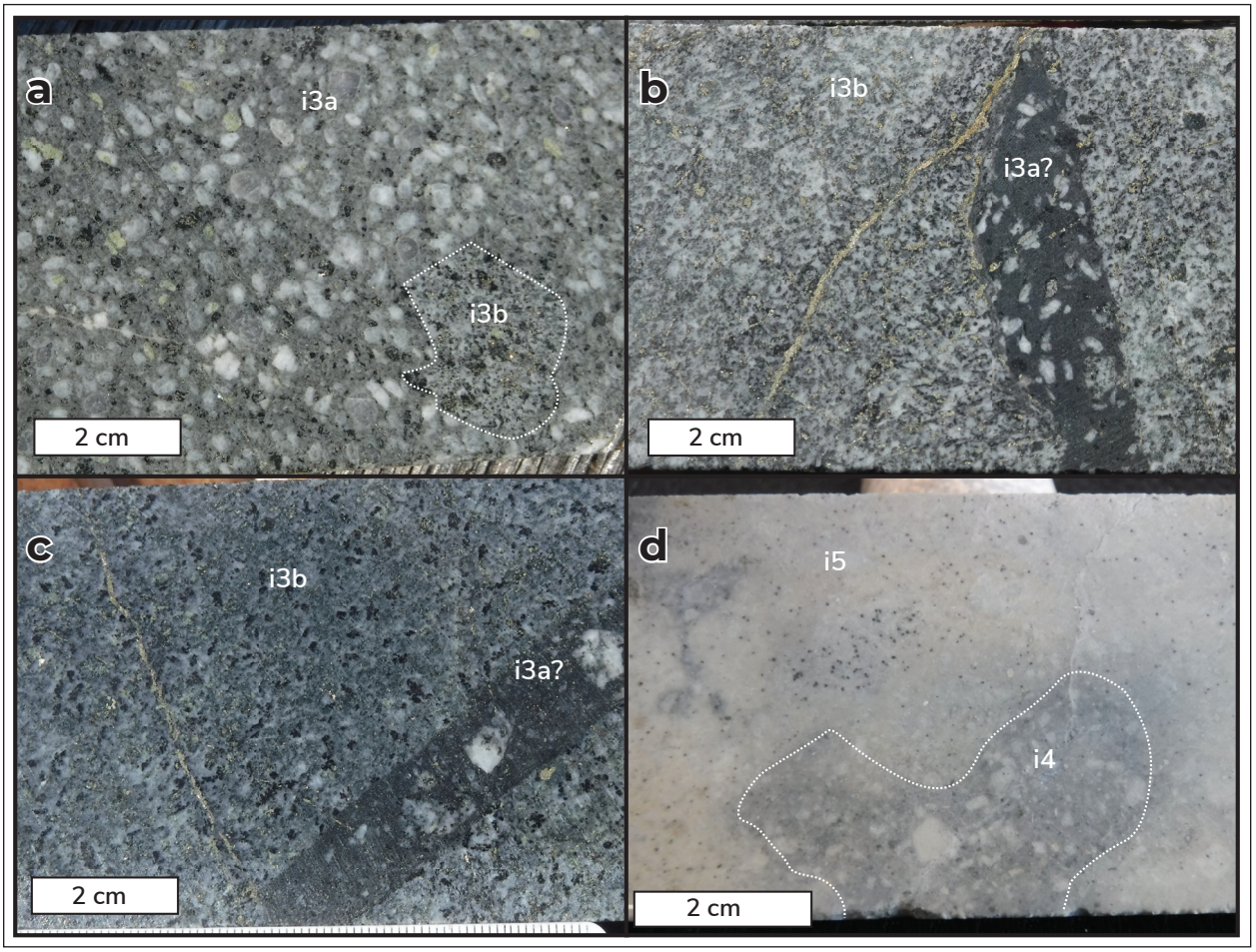

Figure 6. *Crosscutting relationships between intrusive dikes.* ***(a)*** *i3b phase clast within i3a phase.* ***(b)*** *i3a phase clast within i3b phase.* ***(c)*** *i3a phase injection within i3b phase.* ***(d)*** *i4 phase clast in i5 phase.*

Alteration

Phyllic alteration (Porphyry stage)

Quartz-muscovite-pyrite assemblages are associated with Stage 1 (porphyry-type, see below) mineralization in the Klaza system. This alteration can be pervasive and is up to 80 m wide in the southeast part of the deposit. Pyrite and muscovite, the latter verified by X-ray diffraction (XRD), replace biotite and hornblende, whereas K-feldspar is only replaced by muscovite. Plagioclase is minimally altered in this process. Pyrite in this alteration assemblage can be significantly enriched in gold, as seen from elemental mapping (Lee *et al.*, in prep), and may relate to the epithermal fluid overprint. Phyllic alteration in the central Klaza zone yields an ^{40}Ar-^{39}Ar muscovite age of *ca.* 78 Ma (Lee *et al.*, in prep).

Potassic alteration (Porphyry stage)

Potassic alteration is only observed in the southeast part of the deposit in spatial association with stockwork veins related to Stage 1. Potassium staining of altered rocks suggests the addition of hydrothermal-related potassium through growth of minerals such as muscovite, K-feldspar, and biotite; however, detailed mineralogy is needed to verify the potassic alteration minerals, and thus extent in the system.

Epithermal vein-related propylitic alteration

The composite epithermal veins at Klaza are associated with a distinct propylitic alteration halo. This halo, which is wider in the hanging wall of the veins, consists of Fe-carbonate, epidote, and muscovite-illite (both verified by XRD). An important observation of the past field season is that Fe-carbonate, which is now obvious due to oxidation, was not noted in the fresh drill core when originally logged. As the presence of Fe-carbonate reflects proximity to epithermal veins, this observation is significant. It is recommended that carbonate staining (see Hitzman, 1999 for protocol) be used in the future for immediate identification of Fe-carbonate alteration, enabling informed drilling decisions in real time.

Hydrothermal mineralization styles

Stage 1: EDM, A, B, and D-type veins

Several types of veins commonly associated with high temperature magmatic-hydrothermal systems are observed in drill core. Nomenclature used is adapted from Seedorf *et al.* (2005) and Sillitoe (2010) to match observations at the Klaza deposit. Veins are placed in a paragenesis based on relative crosscutting relationships among hydrothermal and magmatic events. Several generations or cycles between the veins are noted and described below.

The earliest veins have two variants: (1) early biotite-pyrite having a K-feldspar selvage (EB-type, Fig. 7a); and (2) early dark micaceous (EDM) infill of quartz ± pyrite ± chalcopyrite having dark haloes (chlorite-biotite; Fig. 7b,c). The haloes are between 4 and 10 cm wide; these veins are only seen in phases i1, i3a and i3b.

A-type veins consist of milky quartz containing pyrite-muscovite, and rarely chalcopyrite. These veins are sinuous and occur in i1 and i3b phases (Fig. 7c). Later A-type veins are planar, sheeted or stockworks, and have an assemblage of granular quartz-pyrite ± chalcopyrite and occur in phase i3a.

B-type veins occur as centre-line pyrite-chalcopyrite veins containing narrow quartz gangue (~1 cm wide) and a distinct K-feldspar (potassic) alteration halo. They occur as planar veins and are present in phases i2, i3a and i3b (Fig. 7d).

D-type veins are common and have many variants in terms of mineral assemblage: (i) pyrite ± quartz ± chalcopyrite; (ii) quartz-tourmaline-muscovite-pyrite ± rhodochrosite; and (iii) quartz-pyrite-muscovite (Fig. 7e). The vein assemblages have distinctive K-feldspar destructive sericite haloes of 8 to 15 cm width. The tourmaline-bearing variant of D-type veins is manifested as a hydrothermal breccia in Central Klaza zone, where intensely sericitized clasts of intrusive rock are cemented by an assemblage of acicular, radial, black tourmaline-muscovite-pyrite-quartz.

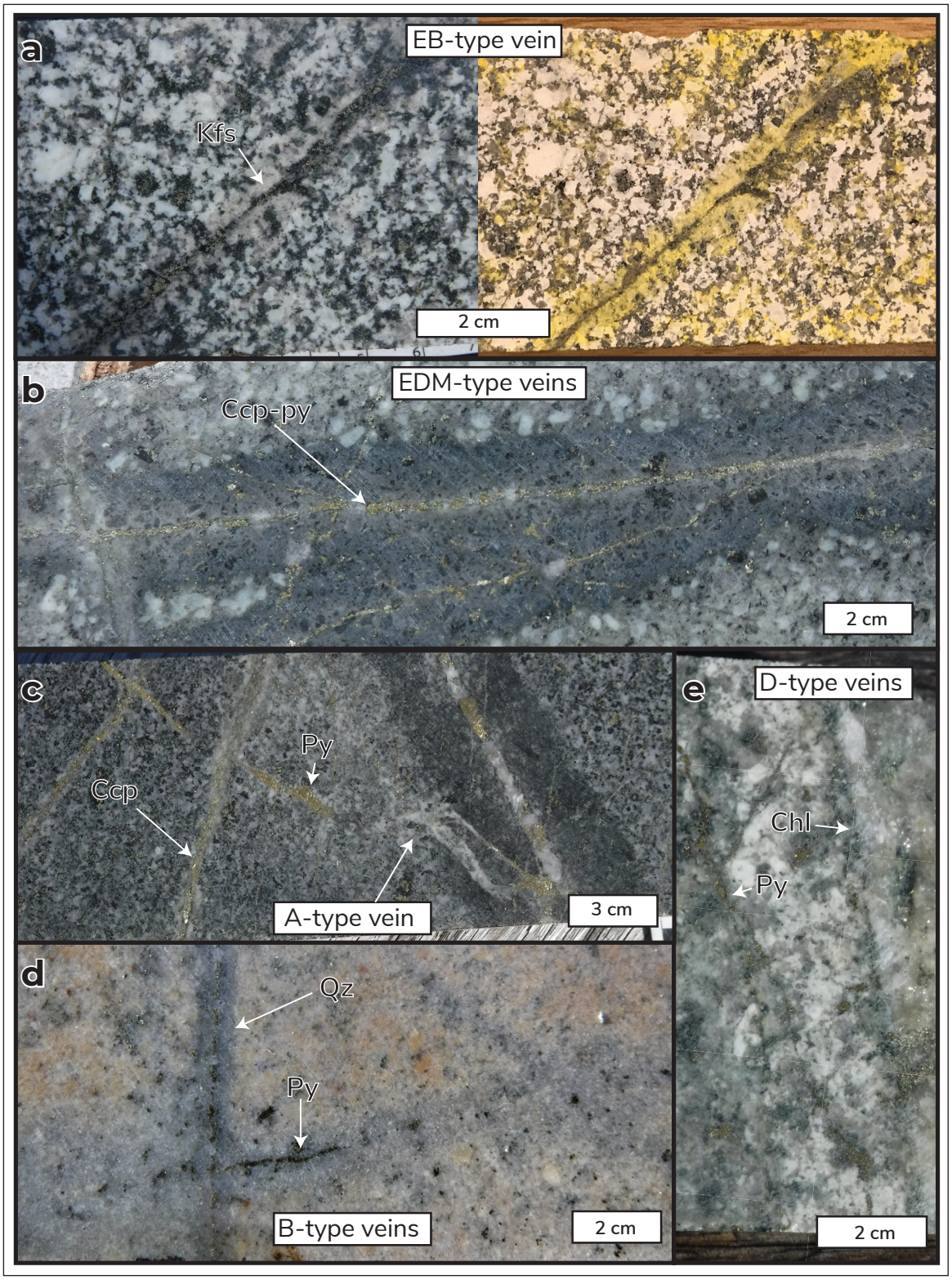

Figure 7. *Porphyry-type veins.* ***(a)*** *Early biotite (EB)-type veins in potassic (biotite) altered i1 phase. Potassium stained slab on the right.* ***(b)*** *Early dark micaceous (EDM) veins hosted in i3a phase.* ***(c)*** *Pyrite-chalcopyrite-bearing A-type veins cutting an EDM vein hosted in i3b phase.* ***(d)*** *B-type pyrite-granular quartz vein with in potassic (K-feldspar) altered i2 phase.* ***(e)*** *D-type quartz-pyrite-sericite veins with texturally destructive muscovite haloes hosted in i1 phase. Mineral abbreviations in accordance with Whitney and Evans (2010).*

Late generation chalcopyrite-only sheeted veinlets cut all vein generations. It is unclear which vein type this generation is associated with; however, it is spatially coincident with disseminated and blebby chalcopyrite mineralization, which occurs by replacing biotite and hornblende in the host intrusive rock. Semi-massive chalcopyrite is also present, which appears to co-precipitate with pyrite (see Stage 2a below).

Molybdenite-bearing veins

Quartz-molybdenite veins are present in the Whitehorse suite granodiorite and have varying alteration haloes. A sample of core from drill hole KL-16-309 is flanked by a strong chlorite-sericite alteration halo; it yielded a Re-Os age of *ca.* 77 Ma (Lee *et al.*, in prep.). A sample from the Cyprus porphyry prospect is flanked by a strong sericitic alteration halo and yielded a Re-Os age of *ca.* 71 Ma (Lee *et al.*, in prep.). One sample obtained from core from drill hole KL-16-314 is cut by epithermal-stage mineralization and is flanked by a narrow carbonate alteration halo; Re-Os geochronological data are pending for this sample.

Stage 2–4: Composite polymetallic veins and breccia

The Klaza composite epithermal veins show a strong structural control. Reactivation of large fault zones is considered to have been an important structural component in creating wide breccia-vein intervals up to 8 m in width. The main breccia-types in the Klaza system are documented below using modified breccia classification systems after Davies *et al.* (2008) and Byrne and Tosdal (2014). The breccia-types are integrated into vein stage descriptions and paragenesis.

Stage 2a veins

Massive fine-grained pyrite-arsenopyrite-quartz ± chalcopyrite veins, 10 cm to 2 m wide, cut Stage 1 veins, and i1, i3a and i4 phases (Fig. 8a). In general, these banded veins have milky white prismatic quartz that is followed by massive sulphide deposition. Pyrite and arsenopyrite from the sulphide substage show equilibrium textures and reflect growth in open space. Gold occurs as: (1) micron-scale electrum inclusions in pyrite, arsenopyrite, and quartz; and (2) lattice-hosted gold in pyrite and arsenopyrite as determined in LA-ICP-MS analysis (Lee *et al.*, in prep). Chalcopyrite, which co-precipitated in this substage, increases in abundance in the Central and Eastern BRX zones.

Stage 2b veins and breccia

This substage is manifested as both banded veins and hydrothermal breccia (C-Bx) — a breccia type characterized by a cement of hydrothermal minerals (quartz, carbonate, sulphide minerals) hosting mono or polymictic clasts. In stage 2b, an assemblage of euhedral arsenopyrite-pyrite-sphalerite nucleated and grew on available surfaces, which are commonly wallrock and clasts of Stage 2a and i4 phase (Fig. 8b). The brecciation event is commonly hydraulic; forming angular jigsaw fit clasts with little displacement or high energy (clast-supported). This substage forms intervals between 5 cm and 1 m wide but can also increase in width as more banding develops (as seen in large vein intersections in the Western BRX zone). This assemblage is followed by cloudy, prismatic quartz, which filled open-space. The cyclical nature of this substage resulted in a banded nature to the composite veins (Fig. 8c).

Stage 2c veins

The final stage of syn-mineralization veins is characterized by prismatic cloudy quartz (possibly from stage 2b), followed by open-space-filling euhedral sphalerite, galena, tetrahedrite-freibergite, minor chalcopyrite and minor dark grey quartz (Fig. 8d). Sphalerite from this substage and Stage 2b is Fe-rich containing compositional zoning, as determined from scanning electron microscopy energy-dispersive X-ray spectroscopy (SEM-EDS) and laser ablation inductively coupled plasma mass spectroscopy (LA-ICP-MS) analysis (Lee *et al.*, in prep). The diversity of sulfosalt minerals in this substage contributes to a large portion of the silver budget in the Klaza system, with significantly higher amounts of sulfosalts present in the Western Klaza Zone; consequently, it is the zone containing the highest Ag:Au ratios on the property.

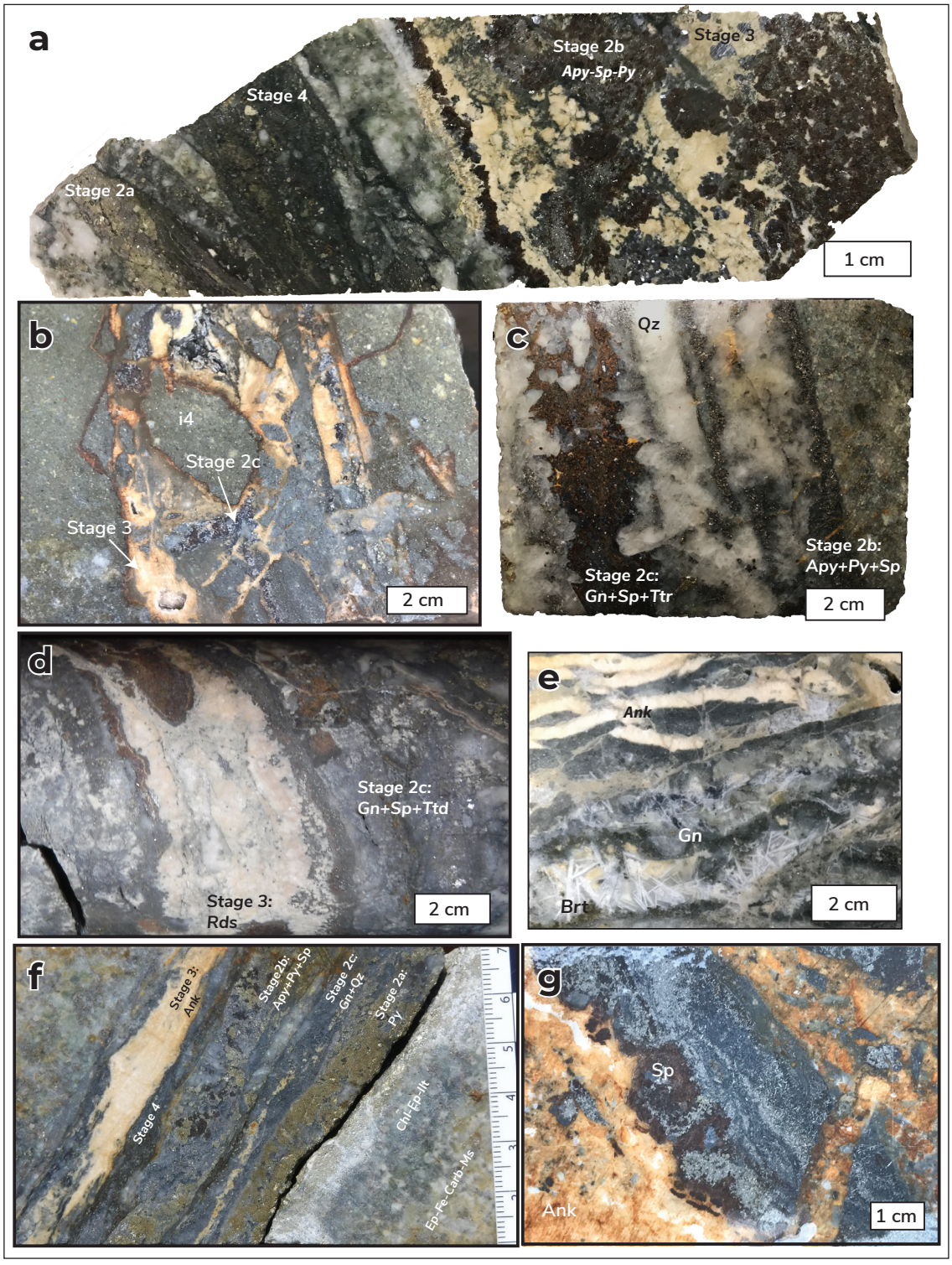

Figure 8. *Epithermal-type composite veins.* ***(a)*** *Western BRX zone Composite vein displaying sphalerite-rich vein stages.* ***(b)*** *i4 phase dikes cemented by Stage 2c and Stage 3 mineralization in the Western Klaza zone.* ***(c)*** *Stage 2b and Stage 2c composite vein form Central Klaza zone in contact with i1 host. Note the banding in Stage 2b and open space fill textures in Stage 2c.* ***(d)*** *Western BRX zone Stage 2c vein cut by Stage 3 rhodochrosite vein.* ***(e)*** *Stage 3 vein from Central Klaza zone displaying banded ankerite and bladed barite.* ***(f)*** *Central Klaza zone composite vein displaying Stage 2 to Stage 4 vein generations generated through reactivation of one structure.* ***(g)*** *Sphalerite–galena–freibergite from Stage 2c brecciated and cemented by Stage 3 ankerite in the Western Klaza zone. Mineral abbreviations in accordance with Whitney and Evans (2010).*

Stage 3 veins and breccia

The carbonate-rich stage cuts and brecciates (C-Bx) all previous vein stages (Fig. 8a,b,d,e,f,g**).** The carbonate in this generation is a solid solution between Fe-rich carbonate (ankerite) to dolomite (Fe, Mg-rich) to rhodochrosite (Mn-rich), as determined by SEM-EDS. This stage contributes minimal base metals to the system and does not display boiling textures (with the exception of bladed barite at ~100 m present depth; Fig. 8e). Brecciation in this stage can be hydraulic (*i.e.*, jigsaw fit; Fig. 8b,g) or high energy, forming small (sub-centimeter sized) subrounded clasts (cement-supported; Fig. 8d).

Stage 4 tectonic breccia-veins

The Klaza epithermal veins show strong evidence of post-mineral fault reactivation, displacement, and brecciation. This matrix-rich breccia (M-Bx) is characterized by the presence of rock flour forming interstitial to clasts of intrusive phases mentioned above, vein material, and other rock types. In the Klaza system, matrix-rich breccia occurs syn to post mineralization (Fig. 9a,b,c), inferred to be tectonic-related breccia and cataclasite. Stage 4 alternates between carbonate-quartz-rich pulses and matrix-rich components, and can result in a combination of matrix-rich and cement-rich breccia (*CM-Bx*). Poorly consolidated fault breccia is also observed within composite veins and in unmineralized fault zones (Fig. 9d).

Other features at Klaza

Magmatic breccia (IG-Bx)

This clast-supported breccia is characterized by an igneous matrix hosting subrounded, monomict to polymictic clasts of intrusive phases noted above plus other clast types. Intrusive breccia has been identified in this study between intrusive generations (i5 containing subrounded clasts of i4; i4 containing rounded clasts of i1) and more uncommon magmatic-hydrothermal composite-type breccia comprising a groundmass of anhydrite, quartz, biotite and feldspar (Fig. 9e). The later breccia-type displays an ambiguous relationship to the main paragenetic vein and intrusive stages defined above.

Tourmaline breccia pipe

A tourmaline breccia pipe is observed in the Cyprus porphyry prospect to the southeast of Klaza (Figs. 1 and 3), where sericitized clasts of porphyritic rock are cemented by black tourmaline-pyrite-quartz-biotite cement (Fig. 9f). This breccia pipe is interpreted to be a hydrothermal breccia related to the Cyprus porphyry complex.

Genetic model

The current compilation of field observations supplemented with a nominal amount of analytical data for the Klaza deposit suggests the composite epithermal veins are part of a much larger scale, continental arc-related magmatic-hydrothermal intrusive complex. Several lines of evidence are discussed below to suggest the presence of a buried Cu-Au porphyry system at Klaza.

1. Magmatic-hydrothermal paragenesis

The magmatic-hydrothermal sequence of events is summarized in Figure 10. Field and supporting petrographic observations suggest cyclical pulses of magmatic and hydrothermal nature analogous to that seen in protracted porphyry systems (Redmond and Einaudi, 2010; Sillitoe *et al.*, 2010). The presence of high-temperature hydrothermal veins (*e.g.*, EDM, A, and B-types) early in the paragenesis conform to classic vein descriptions for porphyry Cu-Au systems (Sillitoe, 2010). In contrast, the epithermal vein substages show a transition from massive sulphide phases, an inferred high temperature massive-sulphide assemblage dominated by pyrite ±arsenopyrite ± chalcopyrite (Stage 2a) to a later, lower-temperature, base metal-rich stage (Stage 2c).

A compilation of currently available geochronological data constrains magmatism (U-Pb zircon), some mineralization (Re-Os molybdenite), and alteration (K-Ar and Ar-Ar for hydrothermal K-feldspar and muscovite) in the Klaza-Mt. Nansen district. The data cluster into two age ranges, both associated with hydrothermal alteration ages (Fig. 11). Initial magmatism between 80 and 76 Ma coincides with the Casino intrusive suite,

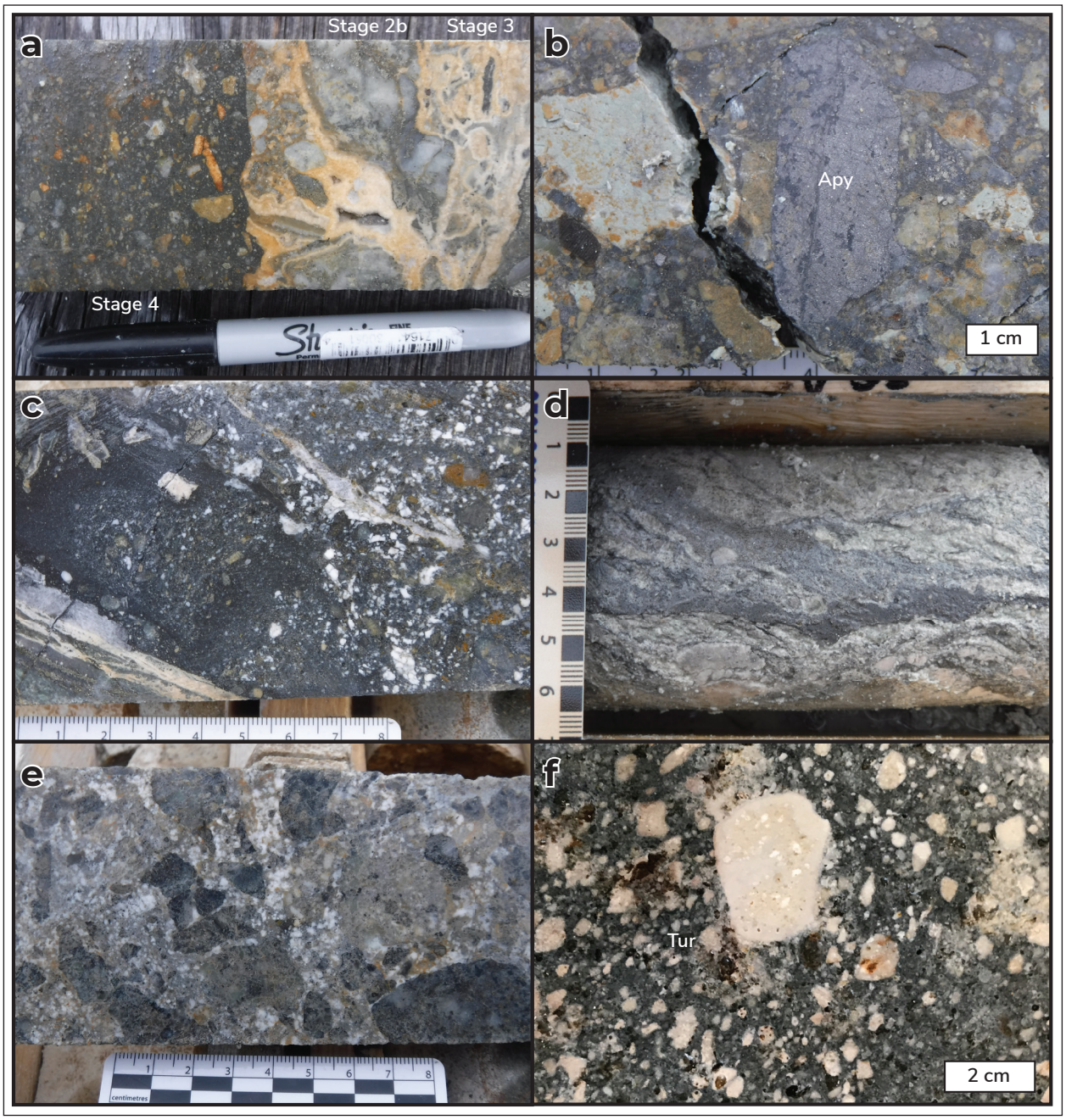

Figure 9. *Breccia types at the Klaza deposit.* ***(a)*** *Stage 4 cement-matrix-breccia cutting a composite breccia of Stage 2b mineralization cut cemented by Stage 3 ankerite.* ***(b)*** *Stage 4 cement-matrix-breccia with polylithic clasts of sericitized porphyritic dike material, i1 host, and massive arsenopyrite from Stage 2a.* ***(c)*** *Cataclasite containing rock flour and barite-carbonate clasts from the Central Klaza Zone.* ***(d)*** *Fault gouge with a brecciated and mechanically sheared sulphide vein.* ***(e)*** *Magmatic-hydrothermal breccia with feldspar-anhydrite cement and polymictic clasts.* ***(f)*** *Tourmaline-cemented breccia from the Cyprus South occurrence with clasts of sericitized porphyritic rock. Mineral abbreviations in accordance with Whitney and Evans (2010).*

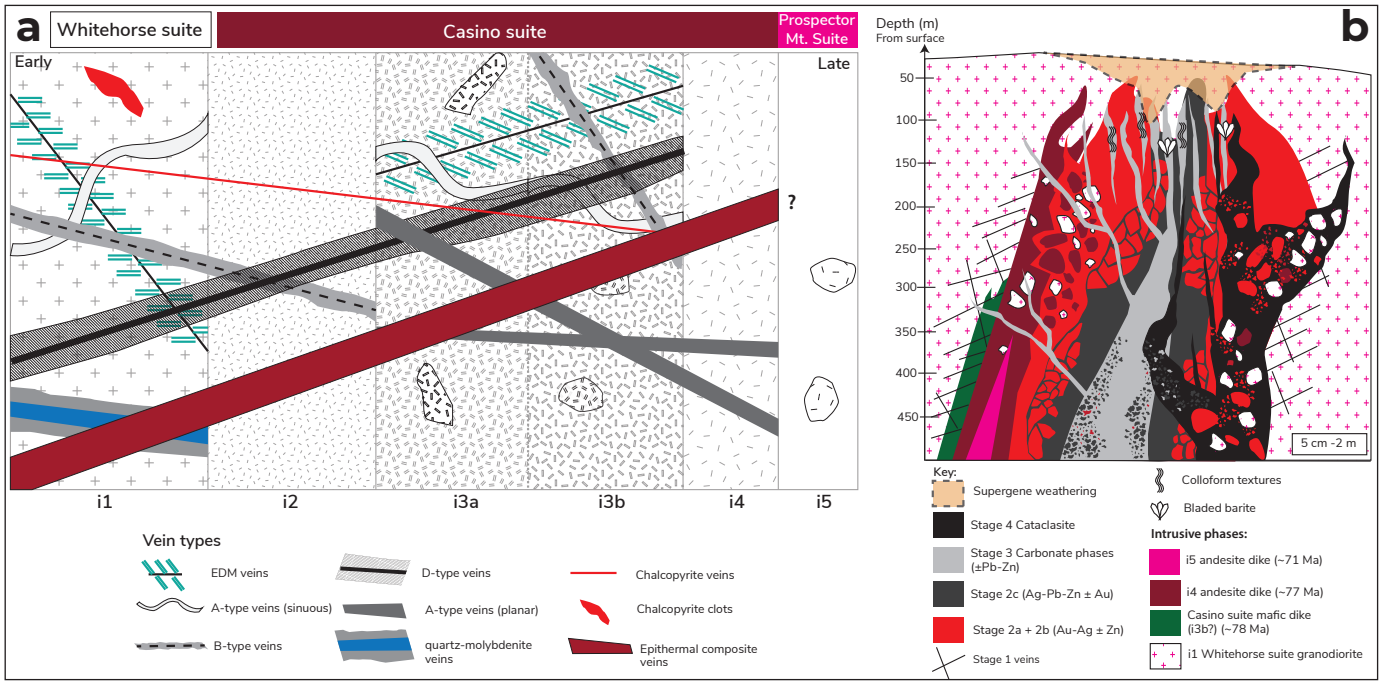

Figure 10. *Magmatic–hydrothermal paragenesis diagrams for the Klaza system.* ***(a)*** *Timeline with crosscutting relationships between magmatic phases and high to low temperature vein types.* ***(b)*** *A schematic diagram of the Klaza composite vein substages and their relationship to magmatic and high-T vein phases.*

which is constrained to ca. 79–72 Ma (Allan et *al.*, 2013). This age range overlaps the 77 Ma molybdenite age for the Kelly prospect and muscovite ages of ca. 79 Ma and ca. 77 Ma for phyllic alteration and tourmaline-pyrite-muscovite vein formation, respectively, at the Central Klaza (Mortensen et *al.*, 2016; Lee et *al.*, in prep). A second magmatic pulse at 72.5 to 71 Ma coincides with the upper age limit for the Prospector Mountain suite, which is constrained to ca. 72–67 Ma (Allan et *al.*, 2013; Friend et *al.*, 2018). The age of this magmatic event overlaps with that of two molybdenite ages of ca. 71 Ma from the Cyprus prospect (Mortensen et *al.*, 2016; Selby and Creaser, 2001a; Lee et *al.*, in prep). K-Ar dates for hydrothermal K-feldspar (*i.e.*, adularia) from an unspecified location in the Mt. Nansen district yielded younger ages of 69 to 68 Ma (Selby et *al.*, 2001b), which also overlaps with the age for the Prospector Mountain suite. In summary, the available age data show a magmatic-hydrothermal system comprising ~10 m.y. arc-related magmatism and an apparent 2 m.y. hiatus. The data support two pulses of porphyry-type mineralization at two locations in the Klaza system, whereby Kelly forms the older, Casino-age porphyry event and Cyprus forms the younger, Prospector Mountain-age porphyry event.

2. Local intrusive rocks

Intrusive rocks of the Casino suite comprise mafic to intermediate compositions that are typical in volcanic arcs. The partially resorbed plagioclase and quartz phenocrysts in the porphyritic rocks (i3a, i4) are indicative of variable P-T-X conditions in the magma chamber, a common feature of productive arc environments and magmatic processes (e.g., Bingham Canyon, Utah; Maughan et *al.*, 2002; Santa Rita, New Mexico; Audetat and Pettke, 2006). The comagmatic mingling of the porphyritic i3a phase and the mafic equigranular diorite (i3b) reflects a dynamic replenishing magma chamber, which is also an important feature of porphyry deposits (Caricchi et *al.*, 2014; Chiaradia and Caricchi, 2017; Putirka, 2017). Thus, there is evidence that the Kelly magmatic system likely experienced chemical changes related to the addition of mafic magma to the magma chamber. The abundance of

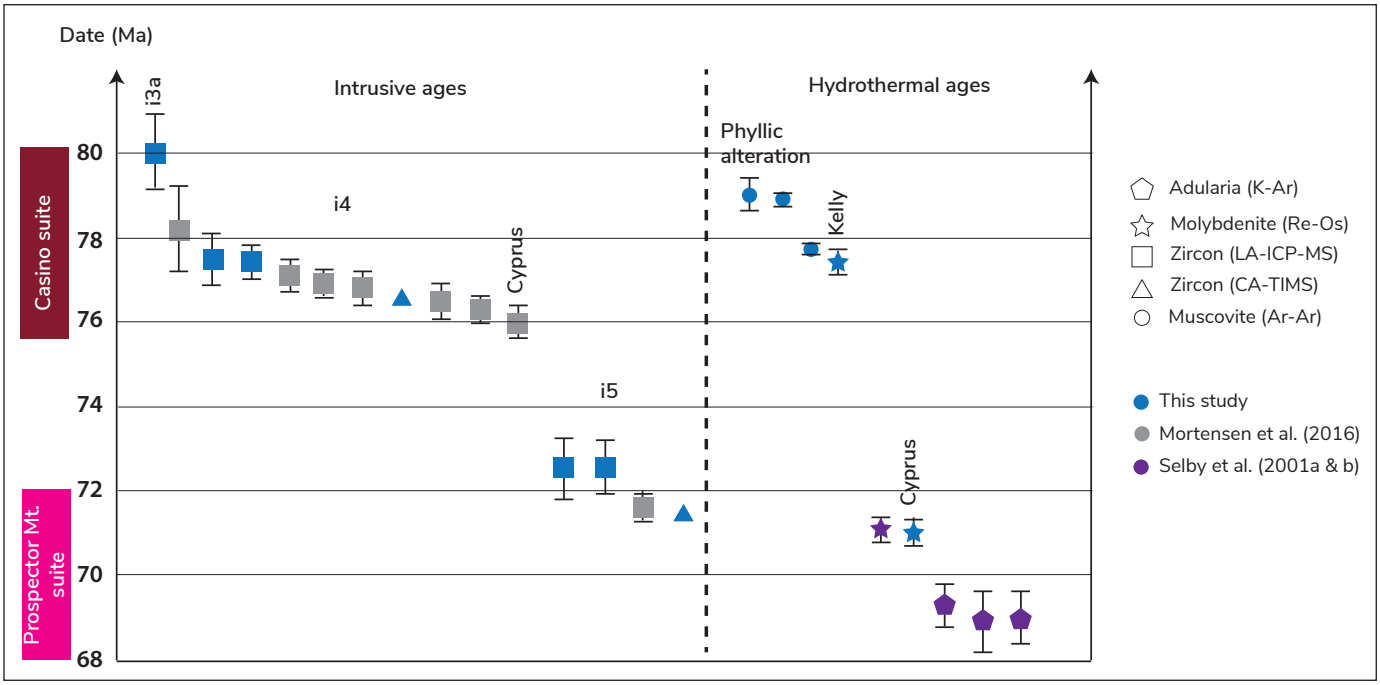

Figure 11. *Summary compilation of geochronologic data from the Klaza deposit area with sources indicated. Casino suite and Prospector Mt. suite boundaries are drawn based on intrusive ages in the Klaza area and in accordance with definitions from Allan et al. (2013). Note that the Selby et al. (2001b) K-Ar data consists of samples with unspecified locations within the Mt. Nansen district.*

hydrous phases, such as hornblende and biotite, in the Casino suite rocks at the Kelly prospect and at Klaza is also characteristic of a fertile (wet) magma chamber and one conducive to form porphyry deposits (Burnham, 1979; Richards, 2011; Richards et al., 2012). Lastly, the variety of porphyritic phases is also a feature typical of many productive porphyry systems (Burnham, 1979; Seedorff et al., 2005; Redmond and Einaudi, 2010; Sillitoe, 2010; D'Angelo et al., 2017).

3. Downhole lithogeochemistry

Three holes drilled southeast of the Klaza deposit resource zone intersected porphyry-type mineralization, and a simplified graphic log for one of these holes (KL-16-314) is summarized in Figure 12. The geochemical signatures of Au, Ag, Cu, K, and Na are split into three domains: (1) epithermal domain (0–200 m); (2) less-altered domain (200–350 m); and (3) porphyry-type domain (350–end of hole).

Distinct, highly anomalous Au, Ag, Cu values that correspond to intersections of composite sulphide-rich veins categorize the epithermal domain. The increase in K and complementary depletion in Na is attributed to muscovite and illite formation in phyllic and propylitic alteration zones related to the epithermal veins. Some barren pyrite-bearing B-type veins were observed in this domain. The less-altered domain displays background values for Au and Cu whereas the uniform K and Na contents reflect least-altered i1 composition. Silver values correspond to minor base-metal bearing veins in this domain. The porphyry-type domain corresponds to an overall above-background Cu-Au response, which correlates to increased vein density (EDM, A, B and D-type veins) and disseminated pyrite-chalcopyrite. It is noted that the potassic (biotite-K-feldspar) alteration assemblage observed in this domain is partially overprinted by phyllic alteration.

Observations of core from drill holes KL-16-314, KL-16-309, and KL-12-134 suggest the current maximum drilling depth (475 m) in the Kelly prospect area intersects the phyllic pyrite ± chalcopyrite bearing shell of a deeper porphyry system.

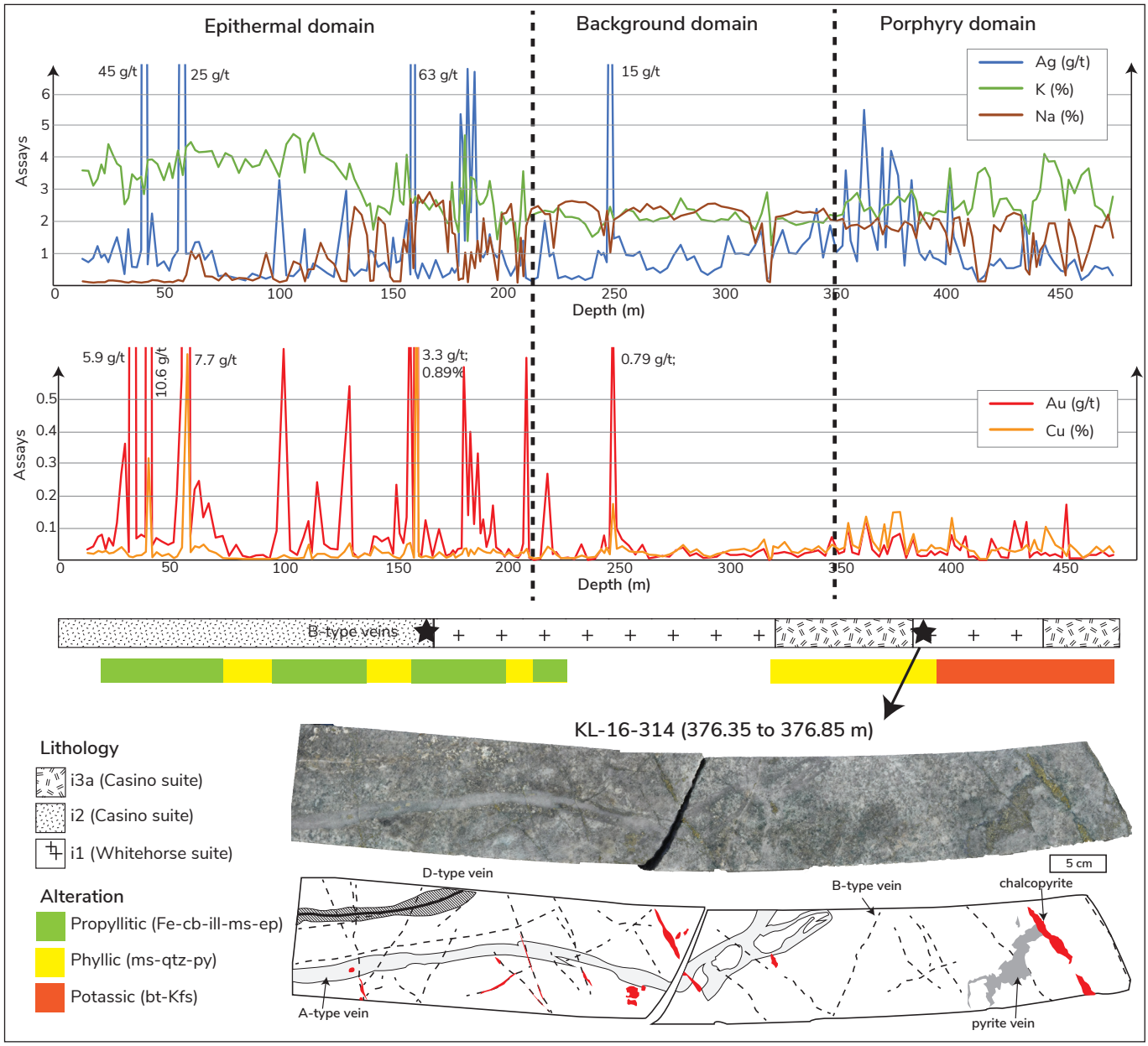

Figure 12. *Graphic log of drill hole KL-16-314 consisting of Au-Ag-Cu-K-Na assay data from Rockhaven Resources Ltd., simplified lithology and alteration re-logs. A representative sample of a A-type vein with crosscutting copper mineralization is also depicted here.*

4. Deposit-scale metal zonation and geophysical data

A schematic summary of the various intrusive suites, mineralization, and geochemistry is illustrated in Figure 13. As seen in Figure 13b, the ca. 76 Ma Casino and later ca. 72 Ma intrusive suites consisting of varied porphyry dike stocks invade the host ca. 105 Ma Whitehorse composite intrusive complex; spatially related to this dike swarm are the epithermal and porphyry-type mineralized zones. The geochemical data from Klaza drill holes display a metal zonation trending from Cu-Au-rich in the southeast (*i.e.*, porphyry-type) to Ag-Pb-Zn-rich (*i.e.*, epithermal-type) in the northwest (Fig. 13b,c). This trend is reflected in the sulphide mineralogy of the composite vein intercepts across the deposit. Intercepts in the

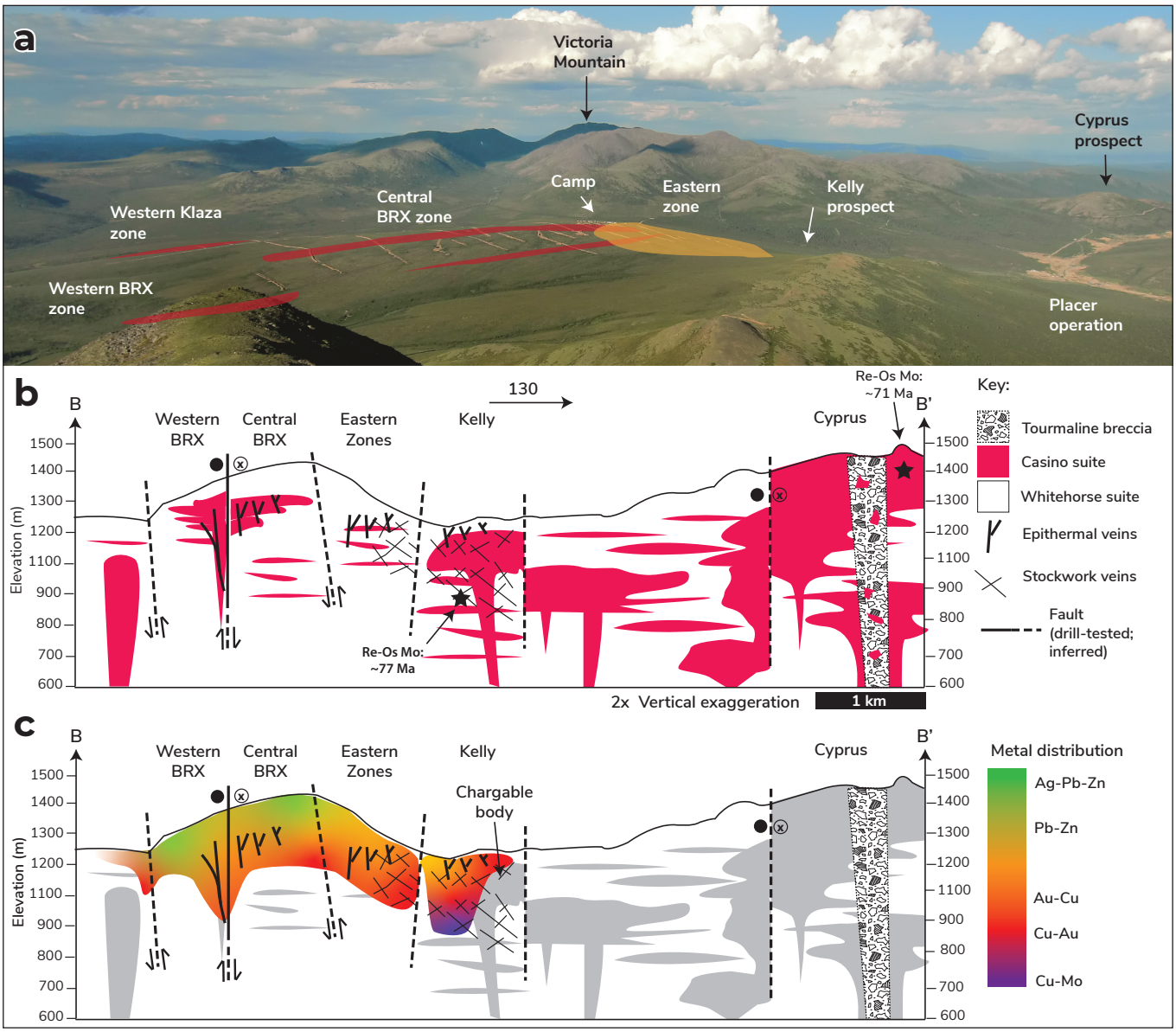

Figure 13. (a) *View of the Klaza deposit looking northeast from the top of Mt. Nansen. Mineralization traces are highlighted in red. Stockwork and sheeted vein mineralization is highlighted in orange.* ***(b)*** *Schematic cross section through B-B' (from Fig. 3a). Relative motion of faults is indicated and inferred based on drill hole and surface data.* ***(c)*** *Section highlighting precious and base metal distribution in the main deposit. Zonation data were obtained from leapfrog models of assay data. The data displayed here are limited to current drilling extents. The location of the chargeable body identified in IP surveys is indicated here and has not been drill-tested. Note that the metal distribution data for the Kelly fault block is only constrained by four drill holes.*

Eastern and Central BRX zones contain significant chalcopyrite hosted in Stage 2a veins, which grades into massive arsenopyrite-pyrite assemblages in the Central Klaza and Western BRX zones. Stage 2a is not present in the Western Klaza zone, and instead contains wider Stage 2c veins with increased sulfosalt abundance and diversity of sulphide minerals.

Induced polarization (IP) geophysical surveys across the Kelly prospect area display donut-shaped high chargeability areas (Fig. 14) coinciding with north-south trending low-resistivity zones (Ross et *al.*, 2018). The high chargeability zones are interpreted to be pyrite-shells while low resistivity zones are interpreted to be clay-altered fault zones.

Exploration Implications

We present a generalized genetic model in Figure 13. The Kelly prospect displays Cu-Au-Mo porphyry potential and requires deeper drill-testing to verify the true economic potential of the inferred underlying system. Archived drill core, on the periphery of current drill pattern, requires relogging by an experienced geologist familiar with porphyry-type geology and mineralization placing an emphasis on generating an updated geological model. This will also generate an appropriate logging scheme to consistently capture relevant information. Thus in regards to this, the new logging scheme should: (1) capture the Whitehorse, Minto, and Casino intrusive suites with the aid of a rock library; (2) record vein types and mineralization on a porphyry-scale in addition to an epithermal scale; (3) record mineralogy-based alteration assemblages; and (4) differentiate between breccia types to aid in resource and metallurgical domain modelling.

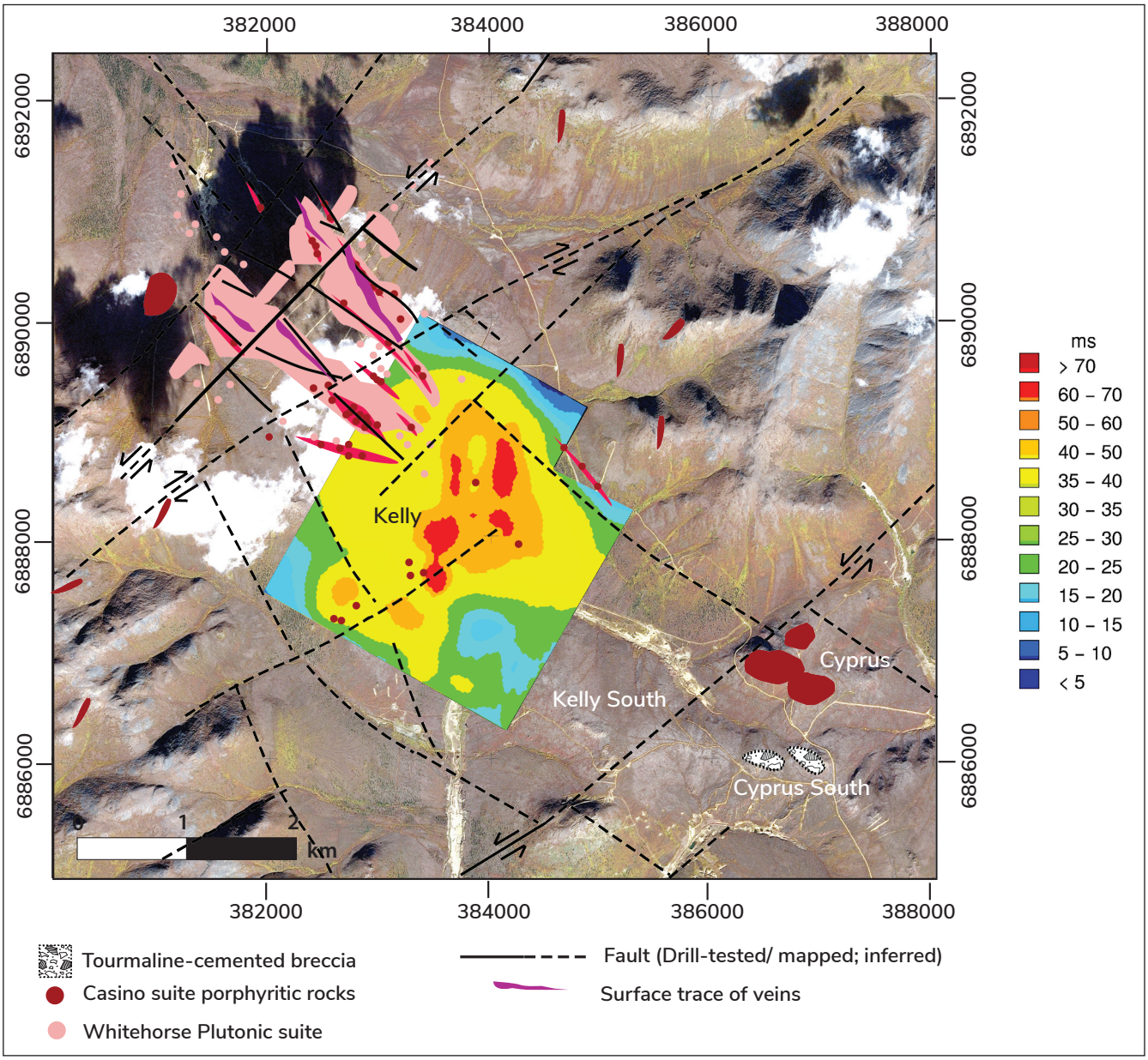

Figure 14. *Induced polarization survey data (chargeability; Ross et al., 2018) from the Kelly zone overlain on an airphoto of the Klaza property. Outcrop and drilling lithologic information is also illustrated for reference to Figure 3.*

IP surveys coupled with airborne magnetic surveys remain important tools for: (1) exploring undercover for large structures, alteration zones, and buried intrusive rocks; and (2) aiding in the reconstruction of geologic maps in outcrop poor areas. The magnetic susceptibilities of the intrusive suites in the Klaza-Nansen area show distinguishable differences, which prove valuable for said map-reconstructions. Note however that fault-related alteration can also significantly lower the magnetic response of these rocks.

Further exploration in the Dawson Range should not discount intrusive rocks outside the prospective 76–75 Ma range from considerations, particularly if said intrusive rocks are porphyritic, contain appropriate abundances of hydrous-mineral phases (hornblende-biotite) and show textural evidence of magma mixing and mingling.

Regional Implications

The longevity and overprinting nature of the magmatic-hydrothermal system at the Klaza deposit also carries implications for understanding the relationship between the Casino (early Late Cretaceous) and Prospector Mountain (late Late Cretaceous) metallogenic events. Although the age of epithermal mineralization at Klaza is currently not directly dated, it is constrained to <76 Ma. Current results show evidence for two overprinting porphyry mineralization events five million years apart. Two contending hypothesis regarding the genesis of the Klaza epithermal veins are to be tested in future work: (1) The Klaza epithermal veins are Casino-age (76–72 Ma) and overprint *ca.* 77 Ma Casino-age Kelly porphyry mineralization during the collapse of the porphyry hydrothermal system, resulting in an epithermal and phyllic overprint of potassic-zone porphyry veins. This is then followed by an overprint from the younger Prospector Mountain-age (72–67 Ma) Cyprus porphyry; or (2) The Klaza epithermal veins are genetically related to the younger Prospector Mountain-age Cyprus porphyry, and form the distal extension of the Cyprus porphyry complex, overprinting the Casino-age Kelly porphyry. Both hypothesis highlight the importance of the late-Late Cretaceous metallogenic event as a significant contributor to precious and base metal endowment in the Dawson Range, Yukon.

Acknowledgements

We are grateful for financial and logistical support from the Yukon Geological Survey (YGS) to conduct fieldwork at the Klaza property. We would like to extend our thanks to Patrick Sack of the YGS for his valuable time, insight and knowledge throughout our time in and out of the field. We also thank Rockhaven Resources Ltd. (RK) for permission to visit and sample at the Klaza property in 2017 and 2019. Matt Turner (RK), Kelson Willms, and Matt Van Loon of Archer, Cathro & Associates are thanked for their time and insight. This paper has greatly benefited from reviews by Patrick Sack and Matt Turner. Work presented in this paper is resultant of the lead-author's on-going PhD thesis at Laurentian University. We acknowledge financial support from the Targeted Geoscience Initiative for the early phase of this study. We also honour the contributions from Jeremy Richards whom is a post-humous co-author, esteemed supervisor, colleague, friend, and technical advisor to RK at the time of his passing.

References

Allan, M. M., Mortensen, J. K., Hart, C. J. R., Bailey, L. A., Sánchez, M. G., Ciolkiewicz, W., McKenzie, G. G. and Creaser, R. A., 2013. Magmatic and metallogenic framework of west-central Yukon and eastern Alaska: Tectonics, Metallogeny, and Discovery: The North American Cordillera and Similar Accretionary Settings. Society of Economic Geologists, Special Publication, vol. 17, p. 111–168.

Audetat, A. and Pettke, T., 2006. Evolution of a Porphyry-Cu Mineralized Magma System at Santa Rita, New Mexico, USA. Journal of Petrology. vol. 47, p. 2021–2046.

Bennett, V., Schulze, C., Ouellette, D. and Pollries, B., 2010. Deconstructing complex Au-Ag-Cu mineralization, Sonora Gulch project, Dawson Range: A Late Cretaceous evolution to the epithermal environment. *In:* Yukon Exploration and Geology 2009, K.E. MacFarlane, L.H. Weston and L.R. Blackburn (eds.), Yukon Geological Survey, p. 23–45.

Bineli Betsi, T. and Bennett, V., 2010. New U-Pb age constraints at Freegold Mountain: Evidence for multiple phases of polymetallic mid to Late Cretaceous mineralization. *In:* Yukon Exploration and Geology 2009, K.E. MacFarlane, L.H. Weston and L.R. Blackburn (eds.), Yukon Geological Survey, p. 57–84.

Bineli Betsi, T., Lentz, D., Chiaradia, M., Kyser, K., and Creaser, R. A., 2013. Genesis of the Au-Bi-Cu-As, Cu-Mo ± W, and base-metal Au-Ag mineralization at the Mountain Freegold (Yukon, Canada): Constraints from Ar-Ar and Re-Os geochronology and Pb and stable isotope compositions. Mineralium Deposita, vol. 48, p. 991–1017.

Burnham, C.W., 1979. Magmas and hydrothermal fluids. Geochemistry of hydrothermal ore deposits, 2nd edition, John Wiley and Sons, p. 71–136.

Byrne, K. and Tosdal, R. M., 2014. Genesis of the Late Triassic Southwest Zone Breccia-Hosted Alkalic Porphyry Cu-Au Deposit, Galore Creek, British Columbia, Canada. Economic Geology, vol. 109, p. 915–938.

Caricchi, L., Annen, C., Blundy, J., Simpson, G. and Pinel, V., 2014. Frequency and magnitude of volcanic eruptions controlled by magma injection and buoyancy. Nature Geoscience Letters, https://doi.org/10.1038/NGEO2041.

Chiaradia, M. and Caricchi, L., 2017. Stochastic modelling of deep magmatic controls on porphyry copper deposit endowment. Scientific Reports 7, article 44523, https://doi.org/10.1038/srep44523.

D'Angelo, M., Miguel, A., Hollings, P., Byrne, K., Piercey, S. and Creaser, R.A., 2017. Petrogenesis and Magmatic Evolution of the Guichon Creek Batholith: Highland Valley Porphyry Cu ± (Mo) District, South-Central British Columbia. Economic Geology, vol. 112, p. 1857–1888.

Davies, A.G.S., Cooke, D.R., Gemmell, J.B. and Simpson, K.A., 2008. Diatreme Breccias at the Kelian Gold Mine, Kalimantan, Indonesia: Precursors to Epithermal Gold Mineralization. Economic Geology, vol. 103, p. 689–716.

Friend, M.A., Allan, M.M. and Hart, C.J.R., 2018. New contributions to the bedrock geology of the Mount Freegold district, Dawson Range, Yukon (NTS 115I/2, 6 and 7). *In:* Yukon Exploration and Geology 2017, K.E. MacFarlane (ed.), Yukon Geological Survey, p. 47–68.

Hart, C.J.R. and Langdon, M., 1998. Geology and mineral deposits of the Mount Nansen camp, Yukon. *In:* Yukon Exploration and Geology 1997, Exploration and Geological Services Division, Yukon, Indian and Northern Affairs Canada, p. 129–138.

Hitzman, M.W., 1999. Routine staining of drill core to determine carbonate mineralogy and distinguish carbonate alteration textures. Mineralium Deposita, vol. 39, p. 794–798.

Klöcking, M., Mills, L., Mortensen, J. and Roots, C., 2016. Geology of mid-Cretaceous volcanic rocks at Mount Nansen, central Yukon, and their relationship to the Dawson Range batholith. Yukon Geological Survey, Open File 2016-25, 37 p. plus appendices.

Kovacs, N., Allan, M.M., Zagorevski, A., Milton, J.E. and Hart, C.J.R., 2017. New geological insights into the Carmacks Copper Cu-Au-Ag deposit, central Yukon (Yukon MINFILE 115I 008). *In:* Yukon Exploration and Geology 2016, K.E. MacFarlane and L.H. Weston (eds.), Yukon Geological Survey, p. 117–140.

Maughan, D. T., Keith, J. D., Christiansen, E.H., Pulsipher, T., Haitori, K. and Evans, N.J., 2002. Contributions from mafic alkaline magmas to the Bingham porphyry Cu-Au-Modeposit, Utah, USA. Mineralium Deposita, vol. 37, p. 14–37.

Mortensen, J.K., Appel, V.L. and Hart, C.J.R., 2003. Geological and U-Pb age constraints on base and precious metal vein systems in the Mount Nansen area, eastern Dawson Range, Yukon. *In:* Yukon Exploration and Geology 2002, D.S. Emond and L.L. Lewis (eds.), Exploration and Geological Services Division, Yukon Region, Indian and Northern Affairs Canada, p. 165–174.

Mortensen, J.K., Hart, C.J.R., Tarswell, J. and Allan, M.M., 2016. U-Pb zircon age and Pb isotopic constraints on the age and origin of porphyry and epithermal vein mineralization in the eastern Dawson Range, Yukon. *In:* Yukon Exploration Geology 2015, K.E. MacFarlane and M.G. Nordling (eds.), Yukon Geological Survey, p. 165–185.

Nelson, J. L., Colpron, M. and Israel, S., 2013. Chapter 3. The Cordillera of British Columbia, Yukon, and Alaska: Tectonics and Metallogeny. *In:* Tectonics, Metallogeny, and Discovery: the North American Cordillera and Similar Accretionary Settings, M. Colpron, T. Bissig, B.G. Rusk and J.F.H. Thompson (eds), Society of Economic Geologists Special Publication 17, p. 53–109, https://doi.org/10.1017/CBO9781107415324.004.

Putirka, K.D., 2017. Down the crater: where magmas are stored and why they erupt. Elements, vol. 13, p. 11–16.

Redmond, P.B. and Einaudi, M.T., 2010. The Bingham Canyon Porphyry Cu-Mo-Au Deposit. I. Sequence of Intrusions, Vein Formation, and Sulfide Deposition. Economic Geology, vol. 105, p. 43–68.

Richards, J.P., 2011. High Sr/Y arc magmas and porphyry Cu ± Mo ± Au deposits: Just add water. Economic Geology, vol. 106, p. 1075–1081.

Richards, J.P., Spell, T., Rameh, E., Razique, A. and Feltcher, T., 2012. High Sr/Y Magmas Reflect Arc Maturity, High Magmatic Water Content, and Porphyry Cu ± Mo ± Au Potential: Examples from the Tethyan Arcs of Central and Eastern Iran and Western Pakistan. Economic Geology, vol. 107, p. 295–332.

Ross, A.A., Kirchner, I., Martin, C.J., Dumala, M.R. and Methven, G., 2018. Technical Report Describing Updated Diamond Drilling, Metallurgical Testing and Mineral Resources on the Klaza Property, Yukon, Canada. NI 43-101, https://doi.org/10.1016/j.cagd.2003.08.001.

Ryan, J.J., Westberg, E.E., Williams, S.P. and Chapman, J.B., 2016. Geology, Mount Nansen–Nisling River area, Yukon. Geological Survey of Canada, Canadian Geoscience Map 292 (preliminary), scale 1:100 000, https://doi.org/10.4095/298835.

Seedorf, E., Dilles, J.H., Proffett, J.M., Einaudi, M.T., Zurcher, L., Stavast, W.J.A., Johnson, D.A. and Barton, M.D., 2005. Porphyry Deposits: Characteristics and Origin of Hypogene Features. In: Economic Geology 100th Anniversary Volume, J.W. Hedenquist, J.F. Thompson, R.J. Goldfarb and J.P. Richards (eds.), Society of Economic Geologists, Inc., p. 251–298.

Selby, D. and Creaser, R.A., 2001. Late and mid-Cretaceous mineralization in the Northern Canadian Cordillera: Constraints from Re-Os molybdenite dates. Economic Geology, vol. 96, p. 1461–1467.

Selby, D., Nesbitt, B.E., Creaser, R.A., Reynolds, P.H. and Muehlenbachs, K., 2001. Evidence for a nonmagmatic component in potassic hydrothermal fluids of porphyry Cu-Au-Mo systems, Yukon, Canada. Geochimica et Cosmochimica Acta, vol. 65, p. 571–587.

Sillitoe, R., 2010. Porphyry Copper Systems. Economic Geology, vol. 105, p. 3–41.

Turner, M. and Dumala, M., 2017. Klaza project: An expanding high-grade Au and Ag resource in the Mount Nansen gold camp (Yukon MINFILE 115I 067). *In:* Yukon Exploration and Geology Overview 2016, K.E. MacFarlane (ed.), Yukon Geological Survey, p. 89–96.

Whitney, D.L. and Evans, B.W., 2010. Abbreviations for names of rock-forming minerals. American Mineralogist, vol. 95, p. 185–187.